

Direct characterization of charge-density-wave defects in titanium-doped TaSe₂ by scanning tunneling microscopy

Xian Liang Wu and Charles M. Lieber

Department of Chemistry, Columbia University, New York, New York 10027

(Received 5 October 1989)

A scanning tunneling microscope has been used to elucidate the effect of impurities on the commensurate charge-density-wave (CDW) phase in a series of Ti_xTa_{1-x}Se₂ materials. Analysis of tunneling images shows that the frequency of CDW defects increases linearly with $x(\text{Ti})$ and that several titanium centers may be necessary to cause a single defect. For $x(\text{Ti}) \leq 0.04$ the localized defects consist of a CDW amplitude distortion, while for $x(\text{Ti}) = 0.07$ defects consisting of a coupled amplitude-phase distortion are also observed. In addition, CDW twin domains that nucleate at these amplitude-phase defects have been imaged in real space for the first time.

The scanning tunneling microscope (STM) has proven to be a particularly useful tool for investigating charge-density-wave (CDW) phases in transition-metal chalcogenide materials since it can simultaneously image the atomic lattice and the charge-density modulation associated with these phases.¹⁻⁷ To date, the STM has been used primarily to characterize the orientation and phase of the CDW relative to the lattice (i.e., the commensurability). Few studies, however, have utilized the real-space imaging capabilities of the STM to address fundamental questions such as how impurities and defects perturb the local CDW properties.^{1,5,7} In this Rapid Communication we report investigations in which the STM has been used to elucidate the effect of impurities on the commensurate CDW phase in titanium-substituted 1T-TaSe₂, Ti_xTa_{1-x}Se₂. We find that the frequency of CDW defects increases linearly with increasing titanium concentration in the commensurate phase. Analysis of this concentration dependence further shows that defects in the CDW structure may be due to titanium clusters rather than isolated impurities. For $x \leq 0.04$ the defects are defined by a reduced CDW amplitude that is localized over 1-2 CDW maxima. The phase of the CDW does not, however, change across these defects. At higher levels of titanium substitution the size of the defects increases and in many cases the CDW undergoes a coupled amplitude-phase distortion across the defect regions. Notably, these amplitude-phase defects are found to nucleate CDW twin domains which have been characterized directly for the first time.

Pure 1T-TaSe₂ exhibits both an incommensurate CDW phase, $473 < T < 600$ K, and a $\sqrt{13}a_0 \times \sqrt{13}a_0$ ($a_0 = 3.48$ Å) commensurate phase, $T < 473$ K.⁸ Previously, DiSalvo and co-workers have used transport measurements to investigate the effect of metal substitution on the incommensurate-commensurate phase transition in $M_x\text{Ta}_{1-x}\text{Se}_2$ materials.^{8,9} They reported that the transition temperature and transition enthalpy decrease linearly with increasing $x(M)$ until, at $x \approx 0.1$, the transition is no longer observed. Suppression of the transition temperature and enthalpy is believed to be due to the random impurity potential which decreases and ultimately eliminates the electrostatic energy gained in forming the commensurate

state. Alternatively, McMillan's Landau calculations suggest that the decrease in transition temperature is due to a stabilization of the incommensurate phase by impurity pinning, and that the commensurate phase, which is already pinned to the lattice, remains essentially unchanged.¹⁰ We have recently used the STM to show experimentally that impurities can pin the local CDW phase in the incommensurate state of 1T-TaSe₂;⁵ however, the local effect of impurities on a commensurate CDW phase has remained largely unexplored.

Single crystals of the $M_x\text{Ta}_{1-x}\text{Se}_2$ materials were grown by chemical vapor transport in a 970 to 900°C temperature gradient over a two-to-three-week period.⁹ The composition and stoichiometry of the materials were verified by elemental analysis. The incommensurate-commensurate transition temperatures for Ti_xTa_{1-x}Se₂ crystals ($x < 0.09$) were determined by variable-temperature resistivity measurements and found to agree with reported values.⁹ In all of these samples the transition temperatures are above 300 K. STM images were recorded at room temperature in the constant-current mode on freshly cleaved crystals using a commercial instrument.¹¹ Data acquisition and analysis procedures have been described previously.^{5,6}

A series of 220×220 -Å gray-scale images recorded at 298 K for $x(\text{Ti}) = 0, 0.02, 0.04$, and 0.07 samples are shown in Fig. 1. In these images both the CDW modulation (wavelength = 12.5 Å) and the atomic lattice (period = 3.5 Å) are resolved. The CDW superlattices observed in images of the titanium-substituted samples exhibit a regular hexagonal structure that is similar to the undoped materials. Bulk resistivity measurements show that for samples with $x(\text{Ti}) \leq 0.08$ the incommensurate-commensurate phase transition occurs above 300 K. These resistivity data thus suggest that the CDW phase is commensurate on average for the doped samples imaged in Fig. 1. For 1T-TaSe₂ the commensurate phase is characterized by a well-defined 13.9° rotation of the CDW superlattice relative to the atomic lattice; in the incommensurate phase this angle is 0°. The commensurate superlattice may be rotated in either a clockwise (β) or counterclockwise (α) direction.⁸ In general, analysis of our STM images shows that the microscopic CDW-

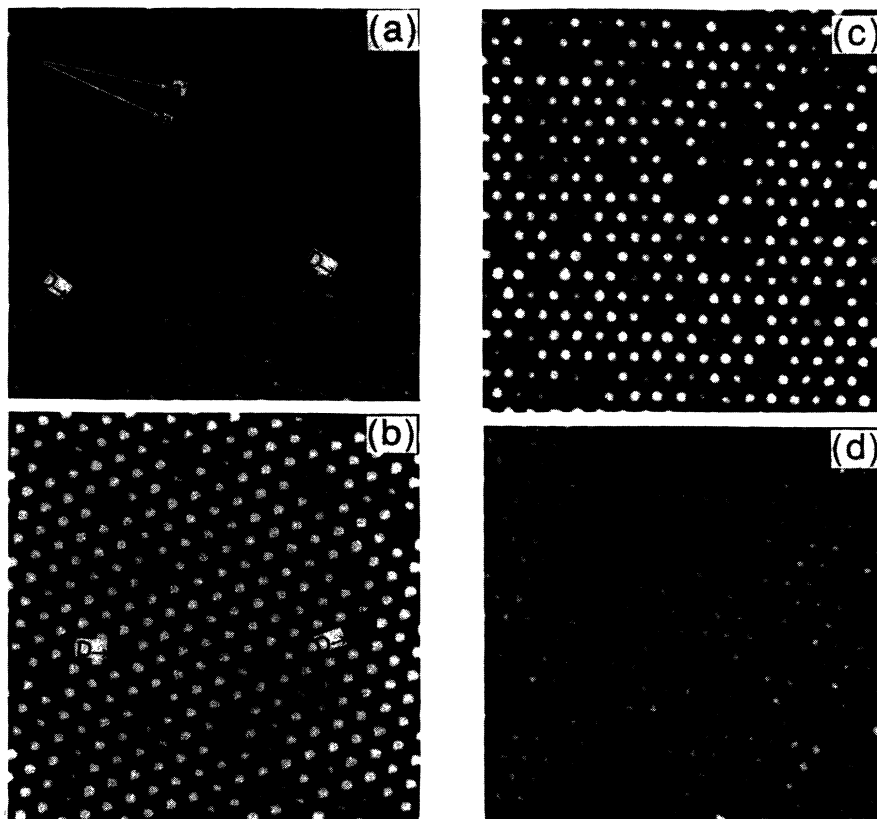


FIG. 1. 220×220 -Å constant-current images of (a) TaSe_2 , (b) $\text{Ti}_{0.02}\text{Ta}_{0.98}\text{Se}_2$, (c) $\text{Ti}_{0.04}\text{Ta}_{0.96}\text{Se}_2$, and (d) $\text{Ti}_{0.07}\text{Ta}_{0.93}\text{Se}_2$ recorded with a 2-nA tunneling current and a 10-mV bias voltage. The lattice and CDW directions are marked by the arrows \mathbf{a} and \mathbf{a}' , respectively, where $\mathbf{a}' = \sqrt{13}\mathbf{a}$ ($|\mathbf{a}| = 3.48$ Å). The angle between \mathbf{a} and \mathbf{a}' is 13.9° . Several CDW amplitude defects are also marked with D 's on the $x(\text{Ti}) = 0$ and 0.02 images.

atomic lattice orientation angle for the Ti-substituted materials is close to the 13.9° value expected for a commensurate phase.¹² Local deviations from a 13.9° angle have, however, been observed in small areas of the $x(\text{Ti}) = 0.07$ images where the CDW amplitude is low.

Further examination of the images obtained for the $x(\text{Ti}) = 0.0$ – 0.07 materials demonstrates that all of these samples have localized regions where the CDW amplitude is reduced relative to the rest of the image. We define these low-amplitude regions to be CDW defects. These CDW defects could arise from surface contamination,⁴ lattice vacancies,¹ or titanium impurities. It is unlikely that localized reductions in the CDW amplitude are due to random surface contamination because (1) the frequency of defects is constant from sample to sample for a fixed titanium concentration, (2) the frequency of CDW defects increases linearly with $x(\text{Ti})$ (Fig. 2), and (3) the atomic corrugation is similar in all regions of the image.¹³ In addition, the surface atomic lattice does not exhibit vacancies or defects in the low CDW amplitude regions and the bulk crystals are stoichiometric to within 1% independent of $x(\text{Ti})$. Hence, it is also unreasonable to attribute these observations to lattice vacancies.¹⁴ We suggest therefore that the CDW defects observed in our STM images are caused by the titanium impurities.

Our data show that the percentage of CDW defects increases linearly with increasing titanium concentration and that the number of CDW defects per titanium impurity, 0.26, is significantly less than 1 (Fig. 2). Notably, this latter result suggests that local CDW defects are not due to single impurities, but rather must be caused by several titanium centers. Other studies of CDW defects in these $\text{Ti}_x\text{Ta}_{1-x}\text{Se}_2$ materials have not been reported, although the CDW structure in the related $\text{Zr}_x\text{Ta}_{1-x}\text{Se}_2$ system has been investigated by neutron diffraction.¹⁵ Analysis of the diffraction data also indicates that several impurities are required to cause a defect in the superlattice. The nature of these defects, however, was not addressed in this previous work.

We have been able to characterize directly the CDW amplitude and phase at these defect sites since both the atomic lattice and CDW superlattice are simultaneously resolved in our tunneling images. For the $x(\text{Ti}) = 0.02$ and 0.04 materials there are 1.5 ± 0.2 and 2.0 ± 0.1 reduced amplitude CDW maxima per defect, respectively. The phase of the CDW on either side of these localized defects is the same, indicating that an amplitude distortion is sufficient to relax the CDW around the impurities. Furthermore, our STM images show that the in-plane CDW phase is coherent over areas at least as large as 10^5

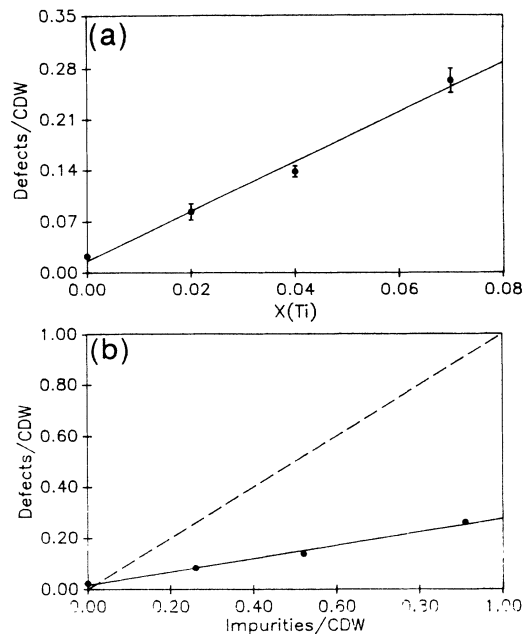


FIG. 2. (a) A plot of the CDW amplitude defects per CDW maxima vs the concentration of titanium. The CDW defects have at least a 1 \AA lower corrugation than the surrounding CDW maxima. The error bars correspond to ± 1 standard deviation determined from the analysis of at least five images per Ti concentration. (b) A plot of the above data vs the number of impurities per CDW maxima. The dashed line corresponds to the hypothetical case in which one impurity causes one defect. The slope of the experimental line is 0.26.

\AA^2 for the $x(\text{Ti}) \leq 0.04$ samples, which is an order of magnitude larger than the coherence area determined by neutron scattering.¹⁵ Since the lower coherence area reported in this scattering study is consistent with the frequency of CDW defects that we observe, it is likely that their results can also be attributed to CDW amplitude distortions rather than phase distortions.

For $\text{Ti}_{0.07}\text{Ta}_{0.93}\text{Se}_2$ samples the CDW defects are significantly larger than in the $x(\text{Ti}) = 0.04$ materials: 4.4 ± 0.6 vs 2.0 ± 0.1 maxima per defect, respectively. More importantly, the defects observed in images of the $x(\text{Ti}) = 0.07$ samples often exhibit a coupled amplitude-phase distortion of the CDW (i.e., the phase of the CDW superlattice on either side of these defects is different). Although the CDW superlattices on either side of a phase distortion could have several possible orientations (e.g., shear dislocations or twinned domains), we have only observed CDW twin domains. In the twin domains the adjacent superlattices are rotated 13.9° clockwise (β) and counterclockwise (α) relative to the lattice, and thus form a 28° angle with respect to each other. Previously, α/β twin domains have been invoked to explain diffraction results,⁸ although our images represent the first real-space characterization of this structure. Two such twin domains are shown in Fig. 3; lines through the CDW's highlight the relative rotation of the two domains. The two-dimensional Fourier transforms of these images, which ex-

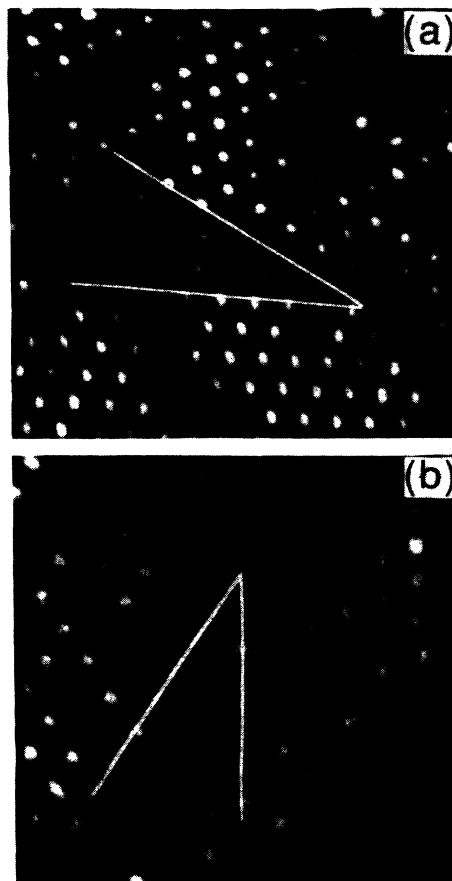


FIG. 3. (a) A $165 \times 165 \text{-\AA}$ image of a $\text{Ti}_{0.07}\text{Ta}_{0.93}\text{Se}_2$ sample that exhibits a CDW twin domain. Lines drawn through the CDW maxima in the two adjacent domains highlight their rotation with respect to each other. (b) A $140 \times 140 \text{-\AA}$ image of a CDW twin domain observed in a $x(\text{Ti}) = 0.08$ sample. The two-dimensional Fourier transform (inset) of this data exhibits 6 first-order lattice peaks and 12 distinct CDW peaks.

hibit six sharp first-order atomic lattice peaks and twelve well-defined CDW peaks, represent an alternative but graphic view of the α/β domains [Fig. 3(b), inset]. The twelve distinct CDW peaks correspond to a superposition of the six CDW peaks from the two superlattice domains that are rotated 28° with respect to each other. Atomic-resolution images further show that the underlying lattice in the twin domain boundaries has no vacancies, suggesting that α/β twin domains nucleate at the titanium-induced phase distortions. Lastly, these observations of titanium-driven defects in the commensurate CDW phase of 1T-TaSe_2 show, in contrast to previous predictions,¹⁰ that a commensurate CDW can be distorted locally by impurities.

In summary, we have used the STM to investigate the local effect of impurities on a commensurate CDW phase. We have shown in a series of Ti-substituted materials, $\text{Ti}_x\text{Ta}_{1-x}\text{Se}_2$, that the frequency of CDW defects increases linearly with $x(\text{Ti})$, and that on average four ti-

tanium impurity centers can be associated with each CDW defect. For $x(\text{Ti}) \leq 0.04$ we have shown that the localized defects consist of a CDW amplitude distortion, while for $x(\text{Ti}) = 0.07$ coupled amplitude-phase distortions are also observed in the defect regions. In addition, CDW twin domains that nucleate at these amplitude-

phase defects have been imaged in real space for the first time

One of us (C.M.L.) acknowledges partial support of this work by The David and Lucile Packard Foundation and the National Science Foundation (CHE-8857194).

¹B. Giambattista, A. Johnson, R. V. Coleman, B. Drake, and P. K. Hansma, *Phys. Rev. B* **37**, 2741 (1988).

²C. G. Slough, B. Giambattista, A. Johnson, W. W. McNairy, C. Wang, and R. V. Coleman, *Phys. Rev. B* **37**, 6571 (1988).

³C. G. Slough, B. Giambattista, A. Johnson, W. W. McNairy, and R. V. Coleman, *Phys. Rev. B* **39**, 5496 (1989).

⁴R. E. Thomson, U. Walter, E. Ganz, J. Clarke, A. Zettl, P. Rauch, and F. J. DiSalvo, *Phys. Rev. B* **38**, 10734 (1988).

⁵X. L. Wu, P. Zhou, and C. M. Lieber, *Phys. Rev. Lett.* **61**, 2604 (1988).

⁶X. L. Wu and C. M. Lieber, *Science* **243**, 1703 (1989).

⁷X. L. Wu and C. M. Lieber, *J. Am. Chem. Soc.* **111**, 2731 (1989).

⁸J. A. Wilson, F. J. DiSalvo, and S. Mahajan, *Adv. Phys.* **24**, 117 (1975).

⁹F. J. DiSalvo, J. A. Wilson, B. G. Bagley, and J. V. Waszczak,

Phys. Rev. B **12**, 2220 (1975).

¹⁰W. L. McMillan, *Phys. Rev. B* **12**, 1187 (1975).

¹¹Nanoscope, Digital Instruments, Inc., Santa Barbara, CA.

¹²The similar trigonal array of atoms at each CDW maxima also indicates that the CDW phase is commensurate (Refs. 1 and 6).

¹³If contaminants were adsorbed on the surface in the low-amplitude regions, then it is expected (in contrast to our observations) that the tunneling probability and thus the atomic configuration in these regions would differ from other areas of the surface.

¹⁴The low frequency of defects detected in the undoped material is probably due to nonstoichiometry in the crystals.

¹⁵D. E. Moncton, F. J. DiSalvo, J. D. Axe, L. J. Sham, and B. R. Patton, *Phys. Rev. B* **14**, 3432 (1976).

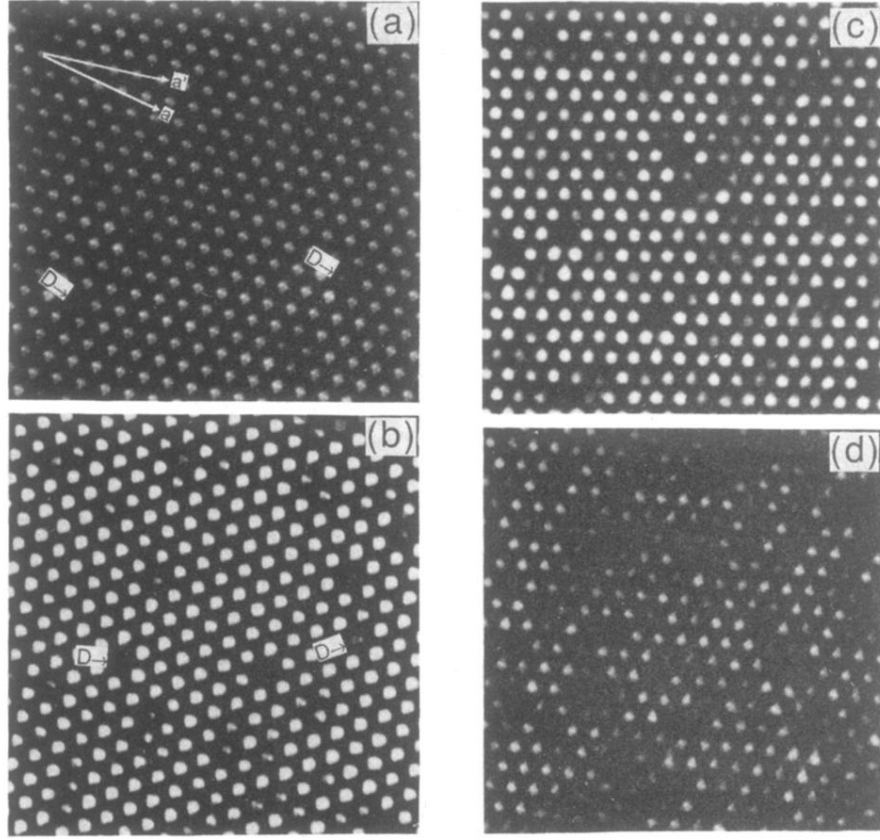


FIG. 1. 220×220 -Å constant-current images of (a) TaSe_2 , (b) $\text{Ti}_{0.02}\text{Ta}_{0.98}\text{Se}_2$, (c) $\text{Ti}_{0.04}\text{Ta}_{0.96}\text{Se}_2$, and (d) $\text{Ti}_{0.07}\text{Ta}_{0.93}\text{Se}_2$ recorded with a 2-nA tunneling current and a 10-mV bias voltage. The lattice and CDW directions are marked by the arrows \mathbf{a} and \mathbf{a}' , respectively, where $\mathbf{a}' = \sqrt{13}\mathbf{a}$ ($|\mathbf{a}| = 3.48$ Å). The angle between \mathbf{a} and \mathbf{a}' is 13.9° . Several CDW amplitude defects are also marked with D 's on the $x(\text{Ti}) = 0$ and 0.02 images.

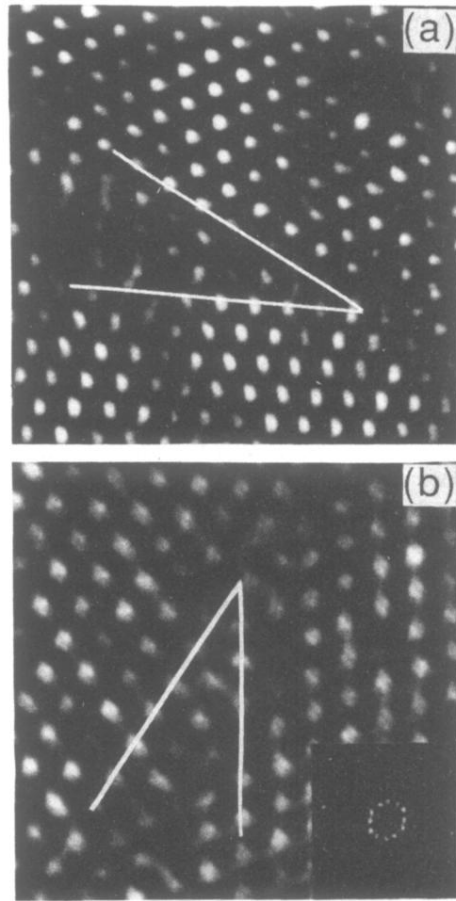


FIG. 3. (a) A 165×165 -Å image of a $\text{Ti}_{0.07}\text{Ta}_{0.93}\text{Se}_2$ sample that exhibits a CDW twin domain. Lines drawn through the CDW maxima in the two adjacent domains highlight their rotation with respect to each other. (b) A 140×140 -Å image of a CDW twin domain observed in a $x(\text{Ti})=0.08$ sample. The two-dimensional Fourier transform (inset) of this data exhibits 6 first-order lattice peaks and 12 distinct CDW peaks.